20th IMEKO TC4 International Symposium and
18th International Workshop on ADC Modelling and Testing
Research on Electric and Electronic Measurement for the Economic Upturn
Benevento, Italy, September 15-17, 2014

RF coupling impedance measurements for particle accelerator devices

Andrea Mostacci[1,4], David Alesini[2], Nicolò Biancacci[3], Fritz Caspers[3], Luca Ficcadenti[4], Joseph Kuczerowski[3], Mauro Migliorati[1,4], Luigi Palumbo[1,4], Benoit Salvant[3], Bruno Spataro[2]

[1]*Sapienza, SBAI Department, Via A. Scarpa 16, 00161 Roma, Italy.*
[2]*INFN-LNF, Via E. Fermi, 40, Frascati (Roma), Italy.*
[3]*CERN, CH-1211 Geneva 23. Switzerland.*
[4]*INFN-Roma, P.le Aldo Moro 2, 00161 Roma, Italy.*

***Abstract* – Bench measurements nowadays represent an important tool to estimate the coupling impedance of any particle accelerator device. The well-known technique based on the coaxial wire method allows to excite in the device under test a field similar to the one generated by an ultra-relativistic point charge. We discuss the basics of the coaxial wire method and review the formulae widely used to convert measured scattering parameters to longitudinal and transverse impedance data. We review, as well, bead-pull technique used in the design, construction and tuning of multi-cell accelerating structures. We discuss typical measurement examples of interest for the CERN Large Hadron Collider as well as other state of the art particle accelerator.**

I. INTRODUCTION

The interaction between a (relativistic) beam and its surroundings is usually described in terms of longitudinal and transverse coupling impedance [1]. The longitudinal impedance accounts for the energy lost by a point charge q because of the wake field of a leading particle; assuming an infinitely long pipe, for a relativistic beam it is defined as

$$Z_{\parallel} = -\frac{1}{q}\int_{-\infty}^{\infty} E_z\left(r=0;\omega\right)\exp\left(j\frac{\omega}{c}z\right)dz \qquad (1)$$

where E_z is the longitudinal electric field and c is the speed of light. Instead the transverse kick experienced by a particle because of deflecting fields excited by a leading charge, can be described in terms of the transverse coupling impedance

$$Z_{\perp} = \frac{j}{q^2}\int_{-\infty}^{\infty} \frac{F_{\perp}\left(r_1,r_2;\omega\right)}{r_1}\exp\left(j\frac{\omega}{c}z\right)dz \qquad (2)$$

where $F_{\perp}$ is the transverse Lorentz force and r_1 (r_2) is the leading (trailing) particle position. Longitudinal impedance is, therefore, measured in Ω while the transverse one in Ω/m.

After the introduction of the beam coupling impedance concept by V. Vaccaro it was realized soon that for highly relativistic beams a very close similarity exists between the TEM like field of the charged particles and the field of a wire in a coaxial structure. This is the basis and motivation of the coaxial wire method.

We review the early concepts of this method in order to show the motivation; we show some issues (and advantages) concerning the practical implementation of those concepts with modern instruments and then eventually we discuss some recent applications.

Longitudinal impedance measurements are straightforward, but also transverse impedance measurements using two wires carrying currents with opposite polarity were already done on the late 70ths. The concept was extended to the evaluation of dipole and quadrupolar impedances by applying a single displaced wire and pair of wires.

We discuss the basis of those methods and present some examples relevant for modern accelerator components.

II. THE COAXIAL WIRE METHOD

The field of a relativistic point charge q in the free space (or in a perfectly conducting beam pipe) is a Transverse Electric Magnetic (TEM) wave, namely it has only components transverse to the propagation direction (z-axis). The amplitude scales inversely with the distance r from the propagation axis and the propagation constant is ω/c. The fundamental mode of a coaxial wave guide is a TEM wave as well, with the same amplitude dependence on $1/r$ and the same propagation constant.

Therefore the excitation due to a relativistic beam in a given Device Under Test (DUT) can be "simulated" by exciting a TEM field by means of a conductor placed along the axis of the structure. The impedance source on the DUT will scatter some field, i.e. exciting some higher order modes; such modes must not propagate otherwise the propagating field will not be anymore similar to the the TEM beam field. In principle, then, simulating the beam field with the TEM mode of a coaxial waveguide is possible only at frequencies below the first higher mode cut-off, namely below the TM_{01} cut-off frequency. One can also demonstrate that the modes of the coaxial waveguide con-

ISBN-14: 978-92-990073-2-7

verges for vanishing wire radius to the analogous mode of the cylindrical waveguide, at least at the beam pipe boundary, where the impedance source is usually located.

To compare the excitation of a given DUT by a coaxial wire and with the beam itself, we are going to discuss some measurements done in the framework of the investigations of the shielding properties of coated ceramic vacuum chambers [2]. The 500 MeV CERN EPA electron beam was sent through two identical ceramic vacuum chamber sections; the first one was internally coated with a layer of 1.5 μm depth (DC resistance of 1Ω). Magnetic field probes were placed to measure the beam field just outside the two ceramic chambers (the coated and the reference one). In a first experiment, shielding properties of the resistive coating (thinner than the skin depth) were demonstrated, confirming previous indirect measurements and simulations [3]. In a following experiment, among other results, it was proved that the screening properties of the coating can be spoiled by the addition of a second conducting layer placed outside the field probes and electrically connected to the metallic vacuum chamber sections. In this case, in fact, the magnetic field probe was measuring clearly the field of the 1ns (r.m.s.) bunched beam (see Fig. 1).

The same chamber in the same configuration (i.e. with this additional external conductor) was then measured in the bench set-up: a 0.8 mm diameter wire was stretched on the axis of the structure. One end of the wire was connected to a 50Ω load while the other end was connected to one port of a Vector Network Analyzer (VNA); matching resistors were used. The other port of the VNA was connected to the field probe. The network analyzer was set to send through the wire a synthetic pulse (time domain option) with 300 MHz bandwidth and measured the transmission between the ports, i.e. the signal through the probe.

This particular kind of set-up is not very often used, but it is very similar to the "time domain" measurement originally proposed by Sands and Rees in the 70s [4]; nowadays time domain measurements are often performed with synthetic pulse techniques in many microwaves applications. The measurement with the beam and with the wire should give virtually the same result, apart from a scaling factor due to the difference of the power carried by the beam and by the VNA signal. The results are shown in Fig. 1 where the beam and the bench data have been normalized and time shifted so that the traces coincides in their minimum point.

The external shield, having a DC resistance much smaller than the coating, carries the image currents, the field penetrates the ceramic and the field probe can measure a clear signal. This is only one of the configurations measured both with the beam and in the bench set-up; the agreement with other measurements is similar to the one of Fig. 1.

The results of that comparison confirm the validity of the coaxial wire approach to simulate the beam field effect on a given DUT. Coaxial wire measurement are widely used to estimate impedances of many accelerator devices. Among many possible examples, we discuss issue of recent measurement on LHC collimators.

A. TCTP LHC collimator impedance measurement

The collimation system of the LHC is one of the largest impedance contributors of the machine, in particular for its transverse imaginary part. In particular, a concern arose for the TCTP tertiary collimator: potentially harmful trapped modes close to 100 and 200 MHz have been found. The effect of the trapped modes depends on the collimator tungsten jaws opening. Detailed simulation and bench measurements have been therefore performed. Eventually proper ferrite absorbers have been designed to try to dump them.

In the TCTP collimator, the main components of interest from a beam impedance reduction point of view are the longitudinal RF fingers that cover the transition from the beam pipe to the collimator structure, the transitions hosting the BPM buttons and the RF system utilizing ferrite blocks and a screen structure as shown in Fig. 2.

In order to match the DUT (i.e. the collimator device) with the VNA, a matching network needs to be designed. The standard procedure requires the knowledge of the DUT transmission line impedance Z_c. In modern network analyzers it is possible to recover this information by means of a time domain reflectometry measurement: the reflection coefficients Γ are measured from both the DUT ports and the corresponding input impedance calculated from

$$Z_c = Z_0 \frac{1+\Gamma}{1-\Gamma}, \tag{3}$$

where Z_0 is usually the 50 Ω cable impedance. Figure 3 shows the characteristic impedance for 3 jaws openings in the collimator: for large gaps, Z_c appears flat, while, for smaller gaps the reflections at the BPM transitions become more and more evident. For practical reasons, therefore, the stretched wire method can be only applied assuming an average value for $Z_c \simeq 230\,\Omega$ taken at the jaws location for intermediate jaws opening. It is moreover interesting to notice how the wire profile could be inferred from the short gap measurements: the flatness of the impedance curve could be used as a wire-based jaws alignment method. The coaxial line characteristic impedance depends, indeed, on the mutual position of the jaws and the wire and the difference between $Z_{1,1}$ and $Z_{2,2}$ is due to difference on the mutual position of the jaws and wire at the two sides of the collimator. Such measurement technique could be used to bench measure the (hopefully small) jaws misalignments with a high level of precision, opening to metrological issues still to be investigated.

The longitudinal impedance can be calculated from the transmission parameters through the improved logarithmic formula [5] and provides an insight on the shunt impedance value in function of the collimator gap. Varying, then, the transverse wire position we can get informations on the TCTP transverse impedance. Figure 4 shows the calculated impedance value for the detected trapped mode at 100 and 200 MHz. The absolute value might not be accurate depending on the field pattern perturbation of the mode due to the wire, nevertheless it is useful for comparisons once the mode damping ferrite will be installed in the TCTP collimator.

III. BEAD PULL TECHNIQUES

An important class of accelerator devices are cavities which are now used both for accelerating and deflecting the particle beam. Each cavity is characterized by its resonant frequency f_0, the quality factor of the resonance Q and its shunt impedance R. One can think of measuring all these quantities with the coaxial wire set-up, i.e. measuring strong notches in the transmission scattering coefficient between the ends of the wire. But the wire perturbs longitudinal cavity modes, e.g. lowers the Q and detunes the frequency. Therefore the coaxial wire set-up is not usually recommended for cavity measurements and it is advisable only for special cases, mainly transverse modes [6].

The most used technique to characterize cavities is the "bead pull" measurement [7]. The field in the cavity can be sampled by introducing a perturbing object and measuring the change in resonant frequency: where the field is maximum (minimum) the resonance frequency will be more (less) perturbed. It is a perturbation method, therefore the perturbing object must be so small that the field does not vary significantly over its largest linear dimension. Shaped beads are used to enhance perturbation and give directional selectivity among different field components.

Quantitatively, the change of the resonant frequency is related to the perturbed cavity field by the Slater theorem. The frequency variation can be measured by the variation of the phase at the unperturbed resonant frequency, according to Ref. [9]. Even if a very precise initial tuning is needed, this method allows easily measuring the field of many points (as many as the points of the instrument trace). The field shape can also be directly visualized on the instrument screen, greatly facilitating the structure tuning procedure.

Novel accelerating devices RF structures foresee a standing wave part is tightly connected to a traveling wave one, thus the Slater resonant approach is not suitable.

Non resonant perturbation theory was first proposed by Steele [10] and allows the measurement of electromagnetic field in the perturbing bead position by measuring the complex variation of the reflection coefficient at a given frequency ω, i.e.

$$\Delta S_{11} = S_{11,p}(\omega) - S_{11,u}(\omega) = -j\omega k_{ST} E^2/P_{inc}, \quad (4)$$

where $S_{11,p}$ ($S_{11,u}$) is the perturbed (unperturbed) reflection coefficient, P_{inc} the average power entering the e.m. structure, k_{ST} a constant and E the electric field at the bead position and at frequency ω. Non resonant perturbation method (in the following referred to as Steele method) is the only way to measure e.m. field in non resonant RF structures through a bead pull technique; it is used in resonant structures when one is interested also in the phase behavior of the field. Equation 4 is written only for electric field, but a more general relation can be found in Ref. [10].

A. *SPARC X-band cavity*

As an example we can consider simulations and measurements done on an 11.424 GHz standing wave multicell cavity, designed for the SPARC photo-injector [11]. The cavity is supposed to work in the π-mode (all the cells are filled with field) exhibiting a maximum field equal in every cell (field flatness). A 9 cells prototype has been designed and built and all the details are reported in Ref. [12] while a picture is given in Fig. 5. We will present measured data against numerical simulation results for the electric field on axis.

Figure 6 compares measured data against numerical simulation results for the electric field on axis. The field has a maximum/minimum in the center of every cell and the tuners have been set to have the required field flatness. The main measurement artifact was the non-negligible effect of the glue used to fix the bead on a plastic wire to be moved by the stepping motor; therefore the glue effect was measured and calibrated away resulting in the data reported in Fig. 6. Numerical codes gives very close results among each other and they all agree well with measurements.

B. *Compact micro-accelerators*

X-band particle accelerators benefit from a reduced size and an higher accelerating field with respect to the standard S-band accelerators, nowadays used for high brightness electron beam production. High accelerating field in X-band, of 200 MV/m peak, allows the production of high brightness beams. We have proposed a design a novel Òhybrid gunÓ from an electromagnetic and beam dynamics point of view together with the low power RF characterization of a preliminary copper prototype of such a gun [13, 14].

The hybrid gun is a structure where the Standing Wave (SW) part hosting the cathode is tightly coupled to the Travelling Wave (TW) section through a coupling cell; a prototype is shown in Fig. 7. Such a device strongly mitigates impedance mismatches, and therefore reflected RF power, during and after the RF filling of the SW section. Therefore no circulator is needed to protect the klystron and this solves the problem of the absence of high power circulator in X-band.

The hybrid gun avoids the bunch lengthening observed during the drift in a split (conventional) photo-injector. The bunch is indeed strongly focused longitudinally through velocity bunching, due to 90° phase shift between SW cell and input coupler. Numerical studies have shown that the emittance compensation dynamics remains manageable even in the presence of strong compression.

We have studied the design of the hybrid gun from an electromagnetic and beam dynamics point of view. Extensive numerical simulations have shown the control of beam size and emittance and the possibility of tuning the working point by changing the temperature of the SW part in the few Celsius degree range. The electromagnetic design has been finalized, according to the most recent design criteria of high gradient accelerating RF structures.

Preliminary field measurement on a first prototype are shown in Fig. 8. According to Eq. 4, the reflection coefficient as a function of the bead position is proportional to the field seen by the particle. The non resonant method allows to characterise both the SW and the TW part.

IV. CONCLUSIONS

In this paper we review the common bench methods to measure coupling impedance for particle accelerator device, both resonant and non resonant. Such methods are widely used nowadays due to characterise most of the devices installed in modern accelerators. we have focused our attention to devices used in state-of-the- art accelerators. Collimators are an open issue for the LHC impedance budget and a careful estimation of their impedance is currently ongoing. On the side of compact accelerators, the X-band technology is currently being investigated as well as innovative RF designs; we have reviewed the measurement techniques needed to bench measure such devices.

V. ACKNOWLEDGEMENTS

This work has been partially funded by EU Commission in the Seventh Framework Program, Contract n. 283745 - CRISP.

REFERENCES

[1] L. Palumbo, V.G. Vaccaro and M. Zobov, in Fifth Advanced Accelerator Physics Course, CAS Cern Accelerator School, CERN 95-06 (1995), p.331. See also INFN LNF-94/041 (1994).

[2] L. Vos, F. Caspers, A. Mostacci et al., CERN AB-Note- 2003-02 MD EPA (2003).

[3] F. Caspers, E. Jensen, F. Ruggiero et al., RF Screening by Thin Resistive Layers, PAC 99, New York (1999).

[4] M. Sands, J. Rees, SLAC report PEP-95 (1974).

[5] E.Jensen, CERN-PS-RF-NOTE-2000-001, (2000).

[6] F. Caspers in Handbook of Accelerator Physics and Engineering, A. Chao and M. Tinger (editors), World Scientific, Singapore (1998), p.570.

[7] R. Rimmer, M. Tinger in Handbook of Accelerator Physics and Engineering, A. Chao and M. Tinger (editors), World Scientific, Singapore (1998), p.403.

[8] T.P.Wangler,Principles of RF Linear Accelerator, John-Wiley and Sons Inc., Canada (1998).

[9] F.Caspers, G.Dome, CERN SPS/85-46ARF (1984).

[10] C.W. Steele, IEEE Trans. on Microwave Theory and Techiniques, MTT-14, Vol. 2, February 1966.

[11] Ferrario M. et al., Nucl. Instrum. Methods Phys. Res. B, 309 (2013), p. 183.

[12] A.Bacci, M.Migliorati, L.Palumbo, B.Spataro, INFN LNF 03/008(R) (2003).

[13] B. Spataro et al, Nucl. Instrum. Methods Phys. Res., A 657, Issue 1, pp. 99-106, (2011); doi:10.1016/j.nima.2011.04.057.

[14] J.B. Rosenzweig et al, Nucl. Instrum. Methods Phys. Res., A 657, Issue 1, pp. 107-113, (2011); doi:10.1016/j.nima.2011.05.046.

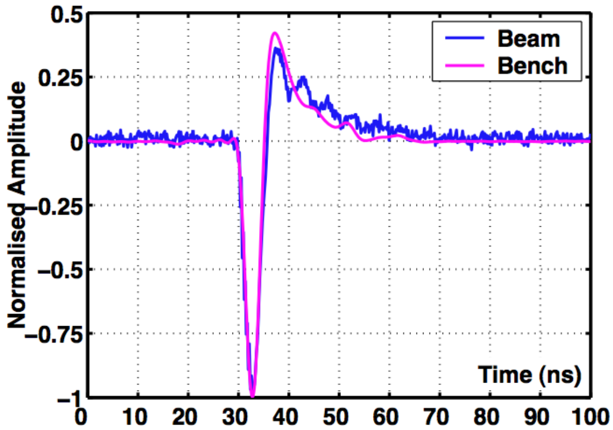

Fig. 1. Signal from the field probe after normalization and time shifting in the EPA experiment on coated chamber shielding properties. The field probe is inserted between the coated ceramic and an external conductor connected to the beam pipe..

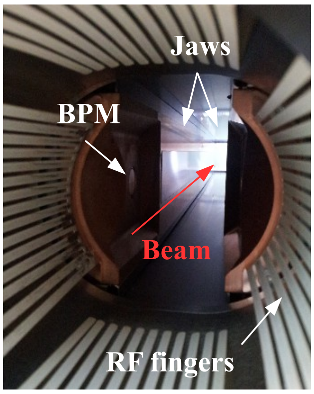

Fig. 2. LHC TCTP collimator internal view: the RF fingers, BPM button and collimator jaws are visible. The wire is stretched along the center of the collimator along the ideal beam trajectory.

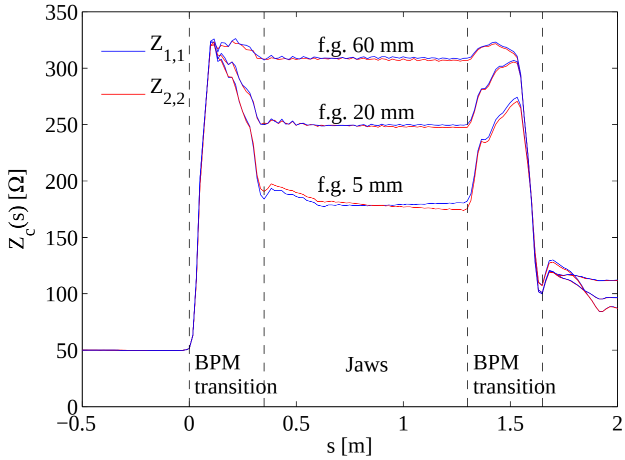

Fig. 3. Transmission line characteristic impedance of the TCTP collimator as a function of length from time domain reflectometry measurement. For short full gaps (f.g.) the BPM transition regions become visible. For larger gaps the impedance becomes flat. The symmetry of the curves from the input ports reflect the DUT symmetry.

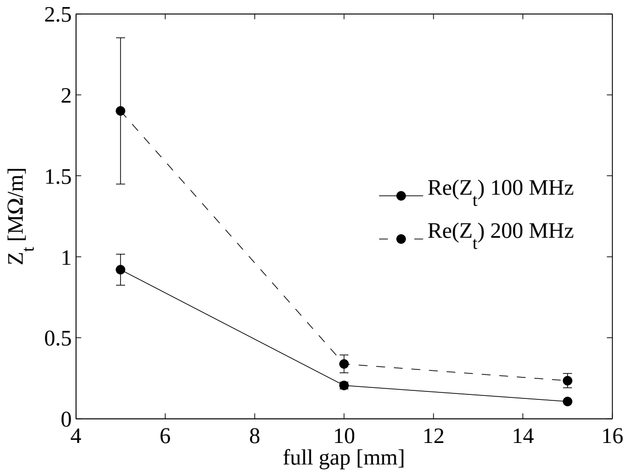

Fig. 4. Peak of the TCTP transverse impedance versus full gap obtained varying the single stretched wire horizontally. The impedance is critical for short gap values.

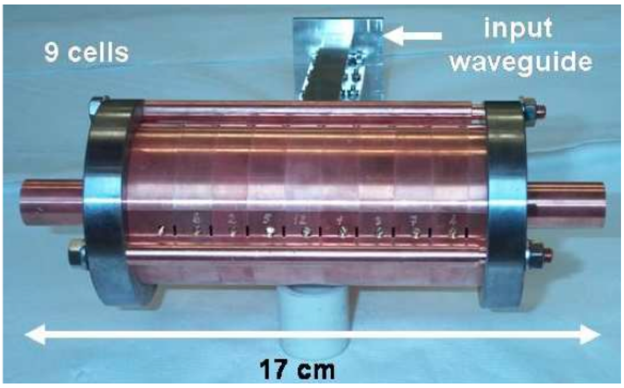

Fig. 5. Nine cells copper prototype of the SPARC 11 GHz cavity.

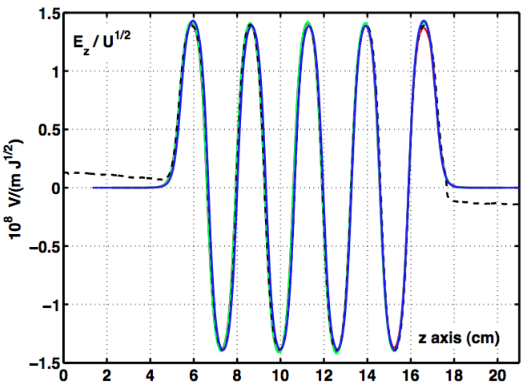

Fig. 6. Longitudinal electric field on the SPARC cavity axis: HFSS simulations (red line), SUPERFISH simulations (green line), MAFIA simulations (blue line) and bead pull measurements (black dashed line).

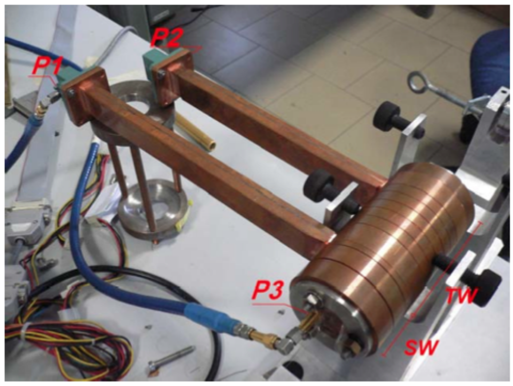

Fig. 7. Prototype of the hybrid gun, where the standing wave (SW) part is tightly connected to the traveling wave (TW) one. The RF power flows from port $P1$ to port $P2$, while port $P3$ is used to monitor the field in the SW cells.

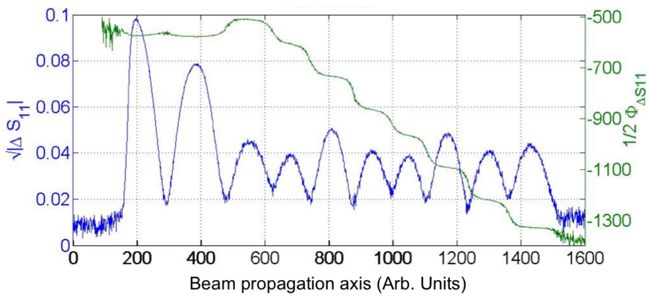

Fig. 8. Longitudinal electric field on the hybrid gun axis measured with the non resonant Steele method.